


# Characterization of the Dynamics of Photoluminescence Degradation in Aqueous CdTe/CdS Core-Shell Quantum Dots

C. G. Pankiewicz<sup>1,2</sup>  · P.-L. de Assis<sup>1</sup> · P. E. Cabral Filho<sup>3</sup> · C. R. Chaves<sup>1</sup> · E. N. D. de Araújo<sup>1,4</sup> · R. Paniago<sup>1</sup> · P. S. S. Guimarães<sup>1,2</sup>

Received: 14 May 2015 / Accepted: 26 July 2015 / Published online: 6 August 2015  
© Springer Science+Business Media New York 2015

**Abstract** We investigate the effects of the excitation power on the photoluminescence spectra of aqueous CdTe/CdS core-shell quantum dots. We have focused our efforts on nanoparticles that are drop-cast on a silicon nitride substrate and dried out. Under such conditions, the emission intensity of these nanocrystals decreases exponentially and the emission center wavelength shifts with the time under laser excitation, displaying a behavior that depends on the excitation power. In the low-power regime a blueshift occurs, which we attribute to photo-oxidation of the quantum dot core. The blueshift can be suppressed by performing the measurements in a nitrogen atmosphere. Under high-power excitation the nanoparticles thermally expand and aggregate, and a transition to a redshift regime is then observed in the photoluminescence spectra. No spectral changes are observed for nanocrystals dispersed in the solvent. Our results show a procedure that can be used to determine the optimal conditions for the use of a given set of colloidal quantum dots as light emitters for photonic crystal optical cavities.

**Keywords** Colloidal nanocrystals · Mercaptosuccinic acid · Emission decay · Photoluminescence · Spectral shift

✉ C. G. Pankiewicz  
cgpanki@gmail.com

<sup>1</sup> Departamento de Física, Universidade Federal de Minas Gerais, Belo Horizonte, MG, Brazil

<sup>2</sup> DISSE - INCT de Nanodispositivos Semicondutores, Rio de Janeiro, Brazil

<sup>3</sup> Departamento de Biofísica e Radiobiologia, Universidade Federal de Pernambuco, 50670-901 Recife, Pernambuco, Brazil

<sup>4</sup> INCT em Nanomateriais de Carbono, Belo Horizonte, Brazil

## Introduction

In the past two decades, semiconductor nanoparticles that behave as quantum dots (QDs) have become an increasingly important resource for biological imaging techniques [1] and, more recently, as a quantum light source [2]. Cadmium telluride (CdTe) was one of the first compounds to be used as an efficient light-emitting nanoparticle, having since become a commercially available product. Its capping with a thin shell of cadmium sulfide (CdS), derived from stabilizing agents containing a thiol functional group (R-SH) or other materials, is widely used as a way of improving photoluminescence efficiency and photostability, shielding the exciton from surface defects and charge fluctuations in the vicinity of a bare nanocrystal [3–8]. Capping with CdS has also been shown to improve biocompatibility [9–11].

While biological applications require that the quantum dots be used in aqueous media [12], their use as sources of quantum light involves either drop-casting on top of photonic structures or controlled deposition using more sophisticated techniques, such as Dip-Pen Nanolithography (DPN) [13]. DPN is particularly suited for quantum optics applications since it allows an accurate positioning of the quantum dots on the photonic structure [14, 15]. As DPN relies on deposition via the water meniscus on an Atomic Force Microscope (AFM) tip, water soluble QDs are very appropriate for use with this technique. Whatever the deposition process, in the end the CdTe quantum dots are put in contact with a solid substrate and the solvent is dried before excitation. This constitutes a very different environment from a cell interior [16, 17] or when the quantum dots are in suspension [18, 19], for example. Since the environment can strongly affect the luminescence of semiconductor nanocrystals [20], the high sensitivity of quantum optics applications to imperfections makes it paramount to have a more complete understanding of how this

environment affects the quality of the emitted light, when one wants to use the quantum dots as a light source for quantum optics applications.

In dry environments, QDs lose their mobility and the formation of clusters is inevitable in the case of drop-casting, in which case the nanoparticles will tend to agglomerate on the rim of a droplet and form a series of high particle-density clusters [21, 22]. Contact with oxygen becomes more significant in case the QDs are used in an open atmosphere and so does laser heating and subsequent thermal effects [16, 23].

While some studies have been conducted on CdTe/CdS QDs in a dry environment [24, 25], a complete picture of phenomena that may happen and how they relate to each other is still lacking. In this work, we perform a systematic study of water-soluble CdTe/CdS QDs, coated with mercaptosuccinic acid (MSA) as a stabilizing/functionalizing agent, in dried droplets. We explore both regions with high and low nanoparticle density, respectively on the rim and close to the center of the dried-out water droplet. We see that the emission intensity decreases exponentially with time under continuous excitation, a behavior that is attributed to the photodegradation of the nanocrystals. We show also that, under low-power excitation, such QDs present a blueshift of their photoluminescence (PL) over time. Conversely, as excitation power increases, there is a redshift of the emission. While both behaviors have been observed separately in previous works by different groups, we show that there can be a continuous transition from one to the other, in the same system. We propose a phenomenological model to account for both blue and red shifts in the photoluminescence.

## Synthesis and Methods

The nanocrystal quantum dots studied in this work were synthesized in aqueous colloidal dispersion by adapting a previously reported method [26]. Briefly, QDs were prepared by the addition of  $\text{Te}^{2-}$  (obtained from metallic tellurium at  $10^{-4}$  mol) in  $\text{Cd}(\text{ClO}_4)_2$  solution (0.01 M) with high pH ( $>10$ ) in the presence of a stabilizing agent, the 3-mercaptopropionic acid (MSA). We used a 5:1:6.0 molar ratio of Cd/Te/MSA. The reducing of metallic tellurium was mediated by sodium borohydride ( $\text{NaBH}_4$ ) in a 1:30 molar ratio of Te: $\text{NaBH}_4$  in a high pH, using NaOH, and under nitrogen saturated atmosphere. The growth of the QDs proceeded under stirring, inert atmosphere and heating at 90 °C during 8 h [27, 28].

The final structure of these nanocrystals is illustrated in Fig. 1a. A CdS passivation layer is formed between the CdTe core and the outer MSA shell due to the thiol group high affinity with cadmium [4, 29]. We confirmed the presence of the CdS layer by XPS (X-Ray Photoelectron Spectroscopy) measurements. We observe the S2p line at 162.0 eV, which is

attributed to the CdS bond [30–32]. Based on the intensities of the S2p, Cd3d and Te3d lines, and considering their sensitivity factors, we estimate the thickness of this CdS layer as two or three atomic layers.

It has been reported that such CdTe/CdS quantum dots should have a type-II band alignment [33]. This would mean that the electrons are more localized in the CdS passivation shell, while the holes are more localized in the core. Figure 1b shows the absorption and emission spectra of the quantum dots dispersed in the solvent, before drop-cast deposition. The narrow emission peak (approximately 25 nm of full width at half-maximum) centered around 647 nm observed in Fig. 1b shows how current aqueous colloidal nanocrystals synthesis techniques can yield QDs with optical quality as good as those diluted in organic solvents [29]. The narrow linewidth of the photoluminescence peak is also an evidence of the charge confinement given by the CdS layer.

The QDs showed an absorption peak at 590 nm. Following Dagtepe et al. [34], we estimate the average diameter of the QDs to be 3.5 nm, as seen in Fig. 1b inset. Transmission Electron Microscopy (TEM) images have confirmed the morphology of the dots. Furthermore, using the coefficient of molar extinction proposed by Yu et al. [35] and Lambert-Beer equations we also estimate the concentration of the QDs from the first absorption peak as approximately 4.0  $\mu\text{M}$ .

In order to analyze the optical properties of the nanocrystals, we drop-cast them on a  $\text{Si}_3\text{N}_4$  surface. As the drop dried, more crystals moved to the rim by diffusion, creating two regions with different densities of nanocrystals, as shown in Fig. 1c.

Microphotoluminescence ( $\mu\text{-PL}$ ) measurements were then carried out with a multimode argon laser focused by a 50 $\times$  objective directly into the dried out drop, at room temperature, in air. Emission spectra were measured using a 0.5 m spectrometer with a 1200 lines/mm diffraction grating and a 256 $\times$  256 pixels CCD.

## Results and Discussion

Firstly, a sequence of  $\mu\text{-PL}$  spectra of the center (low concentration) region of the drop-cast nanocrystals drop on  $\text{Si}_3\text{N}_4$  was taken over time in order to analyze variations with time of the emission intensity of the nanocrystals under continuous excitation. Results are shown in Fig. 2a, for low-power excitation and in Fig. 2b for high-power excitation. A clear exponential decrease of the emission intensity with illumination time was observed, as shown in Fig. 2c and d. The excitation intensity and the spatial position of the laser spot were kept constant during the same set of measurements.

For both high and low excitation powers, the PL intensity decreases exponentially with time, as shown by the exponential fits in Fig. 2c and d. For high power, Fig. 2d, a good fit to

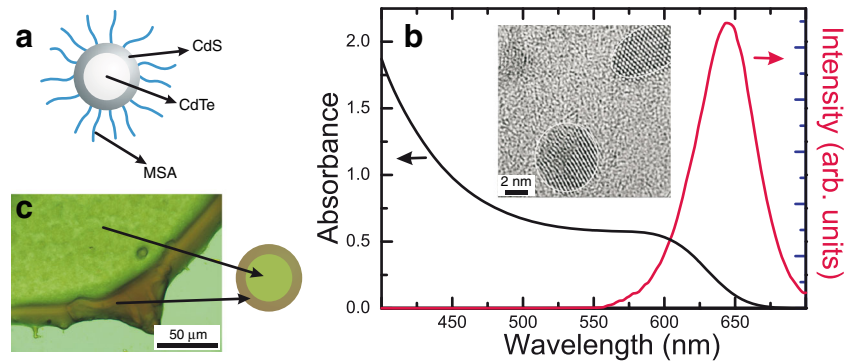


**Fig. 1** (a) Schematic diagram of the nanoparticles under study, composed of a CdTe core enveloped by a layer of CdS and mercaptosuccinic acid (MSA). (b) Optical absorption and photoluminescence spectra of the CdTe/CdS nanocrystals dispersed in the solvent. Inset: A Transmission Electron Microscopy (TEM) image of the nanoparticles. The black bar at the bottom left corner stands for

2.0 nm. When dropcast, these particles agglomerate on the peripheral region of the deposited drop, leaving its center with a low nanoparticle density, as illustrated in (c) by a microphotograph of one such dried drop. The green tint in the image is given by the reflection of white light on a thin layer of Si<sub>3</sub>N<sub>4</sub> used as substrate

the decay is obtained only with a double exponential. In addition to the intensity decay, a small, but clear, shift of the emission spectra was observed. The spectral shift of the PL with illumination time is quantified in Fig. 2e for low excitation power and in Fig. 2f for high excitation power, where, after a Gaussian fit of the PL spectra, the center wavelength of the emission is plotted as a function of excitation time. For the low-power excitation a blueshift is observed while high-

power excitation induces an emission redshift. Similar measurements were performed for a wide range of excitation intensities, with similar results.

In order to follow the regime change from blueshift to redshift of the spectra, the emission of the center region of the drop on Si<sub>3</sub>N<sub>4</sub> was measured for different excitation intensities. To quantify the wavelength shift for a given excitation intensity, a set of μ-PL measurements was taken, with an

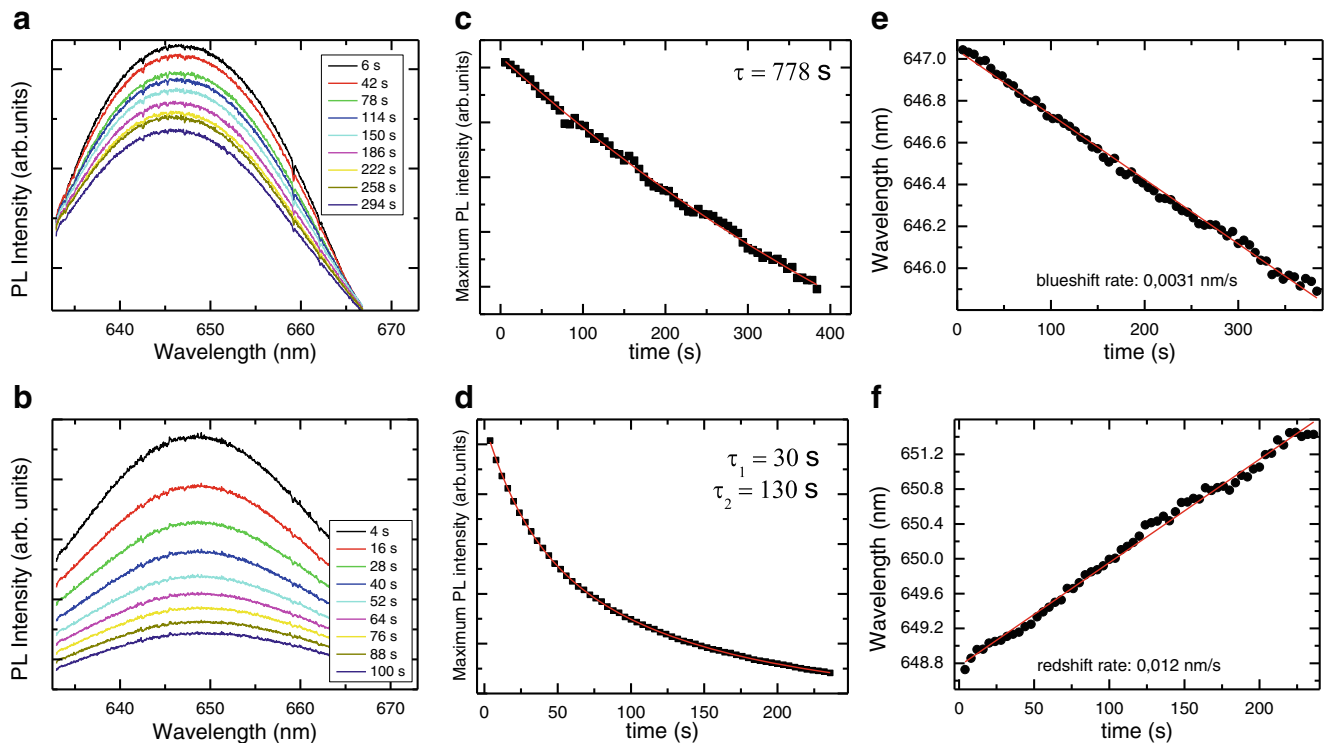


**Fig. 2** Sequence of μ-PL spectra taken over time for (a) low-power excitation, 5.3 kW/cm<sup>2</sup>, and (b) for high-power excitation, 75 kW/cm<sup>2</sup>. Panels (c) and (d) show the evolution with time of the intensity maximum for the low and high power excitations, respectively. The lines are

exponential fits to the data, with the decay times indicated in the figure. The respective shift with time of the central wavelength of the luminescence is shown in (e) for the low power excitation and in (f) for the high power excitation

interval of 3 s between each measurement, up to a total exposition time of 300 s. The integration time for each measurement was 1 s. The position of the laser on the sample and its power were kept constant over the whole exposition time (300 s). We define  $\Delta\lambda$  as the difference between the center wavelength of the emission in the last spectrum of the set (300 s of laser exposure) and in the first spectrum (1 s exposition time). Afterwards, the position of the laser spot on the sample was slightly changed and the same procedure was repeated for the next value of excitation intensity. Therefore, for each excitation intensity a fresh set of nanocrystals was being excited. Figure 3a shows how  $\Delta\lambda$  determined in this way changes with excitation intensity. A regime change from blueshift to redshift is seen at excitation intensity around 30 kW/cm<sup>2</sup>.

To test the reversibility of those spectral shifts, a sequence of  $\mu$ -PL spectra with increasing excitation power was taken rapidly (integration time of 1 s) over time, at the same spot at the center of the drop deposited on Si<sub>3</sub>N<sub>4</sub>. After reaching 70 kW/cm<sup>2</sup> the power was then lowered continuously, to verify if the emission would shift back to its previous wavelength. Figure 3b shows that once entered the redshift regime at high excitation intensities, a subsequent decrease of laser power does not recover the low-power emission spectrum; a permanent change in the nanocrystals emission occurs.

As our results show, the spectral shifts happen simultaneously to an exponential decrease in photoluminescence intensity over time [36]. It is possible to observe both a blue and a red shift in the emission from the same system of quantum dot nanoparticles, by varying the excitation laser power. These distinct phenomena indicate that the interaction of CdTe/CdS nanocrystals deposited on Si<sub>3</sub>N<sub>4</sub> with light is more complex than simply absorption and emission of photons by artificial atoms, and involves a combination of processes, which we shall now discuss in more detail.

Firstly, both the exponential decrease in photoluminescence intensity and the wavelength blueshift are related to the same process of photo-oxidation of the CdTe core, even though a shell of CdS is present [37, 38]. We believe this to be due to diffusion of oxygen through defects on the shell crystal structure [39]. The processes behind the redshift itself were found to be a combination of nanocrystals agglomeration [12, 40] and thermal effects [18], as discussed below. As both these phenomena are more pronounced as the laser intensity progressively increases, the redshift prevails for higher intensities.

At least part of the observed redshift can be related to simple thermal expansion of the nanoparticles. The data from this low-nanocrystal-concentration region of the dried drop are consistent with a temperature increase of at most 10 K above room temperature [41, 42]. This is in fact the maximal expected thermal effect of a focused laser for the powers and spot size used in our experiments, given dissipation through contact with the Si<sub>3</sub>N<sub>4</sub> substrate which we suppose remains at room temperature for regions more than 5  $\mu$ m away from the laser spot. Nevertheless, a small *irreversible* redshift was observed, indicating that another process must be involved. Given that temperatures are not sufficiently high for any sort of surface reconstruction to take place, we suggest that the process causing the irreversible redshift demonstrated in Fig. 3b is a progressive agglomeration of nanoparticles induced by the high intensity laser exposure. As the distance between the nanocrystals diminishes, the exciton wave function will become delocalized between neighboring nanocrystals, leading to a decrease in confinement and thus to a decrease in the recombination energies. We note that a type II band alignment as suggested by Dai et al. [33] would favor this hypothesis. In this case, electrons would be more localized in the shell and nanocrystal agglomeration would lead to an effective increase of the electron quantum well. A

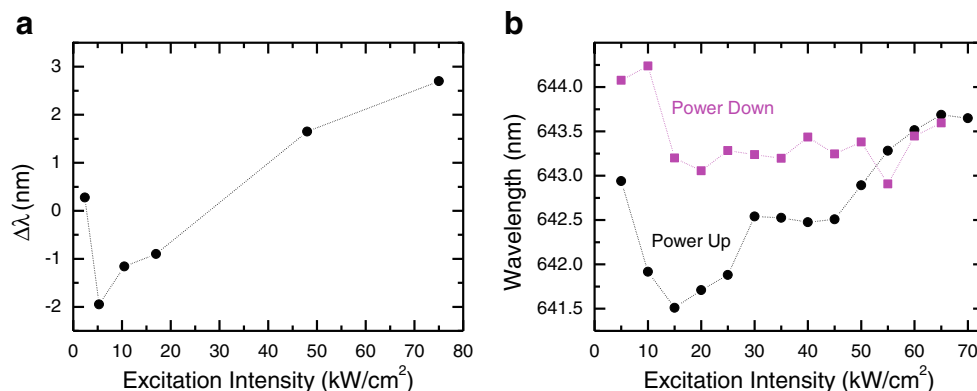


**Fig. 3** As the excitation intensity changes, the spectra of the nanocrystals deposited on Si<sub>3</sub>N<sub>4</sub> shift. Panel (a) shows the shift in the central wavelength of the emission after illuminating for 300 s with each excitation power. Each point in the graph was obtained in a slight different spatial position at the center of the dried drop of nanocrystals.

Panel (b) shows the instant wavelength variation, i.e., the laser spot was kept at same point for all excitation power intensities and the spectra was recorded with a 1 s accumulation time. To minimize nanocrystals degradation, the laser was blocked between the changes in laser power

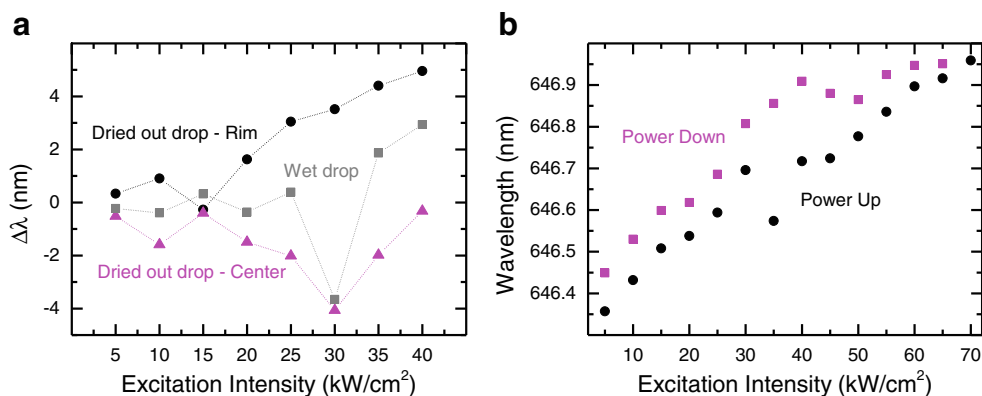


**Fig. 4** a: Spectral shift after 300 s laser exposure time ( $\Delta\lambda$ ) as a function of excitation intensity, for nanocrystals deposited on  $\text{Si}_3\text{N}_4$  by drop-cast (Center), for a just deposited drop (Wet drop) and at the border of a drop (Rim). For each intensity the laser spot is repositioned slightly, so every measurement is taken over a fresh set of nanoparticles. b: Absolute

change in the central wavelength of the emission with increasing excitation intensity for a region in the rim of the dried out drop. Measurements were taken in the same spot of the drop, with 1 s integration time. To avoid severe deterioration of the nanocrystals, the laser was blocked between each measurement

redshift can also be produced by a transfer of excitons from small size to larger QDs [43], a process that is also favored by the agglomeration of the nanoparticles.

To fully understand the aforementioned processes additional measurements were made, at regions of different concentrations of nanocrystals inside the dried drop deposited on  $\text{Si}_3\text{N}_4$ . The results are shown in Fig. 4. Plots of the wavelength shifts,  $\Delta\lambda$  (determined in the same way as in Fig. 3), as a function of power intensity are shown in Fig. 4a for different concentration regions in a drying drop deposited on  $\text{Si}_3\text{N}_4$ . Some  $\mu$ -PL spectra were taken before the drop dried out completely, i.e., in a wet drop, where the nanocrystals concentration and dispersion are closer to their original values in suspension. After the drop dried out, measurements were taken at its center and also at the drop rim. The center region of the dried out drop behave in accordance with the results discussed above, i.e., a blueshift regime and then a redshift regime are observed with increasing laser power. However, the blueshift regime is not observed for the rim, where the nanocrystals concentration is significantly higher and there is water present. The wet drop displays an intermediate behavior.

For the high-concentration region, located at the rim, besides the absence of the blueshift regime, the induced redshift was found to be reversible, as indicated by Fig. 4b. These results suggest that at the rim the nanoparticle agglomeration occurs at a slower rate, likely due to more water being present at this region. This makes the nanoparticles thermal expansion the main mechanism responsible for the redshift. The reversibility of the redshift in those circumstances also indicates that size-selective mechanisms such as reactive photolysis does not play a relevant part on the observed spectral shifts.

In the center of the dried droplet, a region of low concentration of nanocrystals, as the spectra changes to a redshift regime at higher excitation powers as described above, the

emission intensity maintains its behavior of exponential decrease with illumination time. This can be explained by the underlying presence of the photo-oxidation mechanism, which leads to a blueshift but is dominated at high powers, as far as the spectral shift is concerned, by the redshift-inducing processes. The photo-oxidation of the nanocrystals should occur at all excitation powers, and continue to degrade photoluminescence by increasing the probability of a faster non-radiative relaxation. This is supported by data obtained in a dry  $\text{N}_2$  atmosphere, for which blueshifts were not observed for low concentrations and the decay rate of the photoluminescence was lower than that in an open atmosphere, as shown in Fig. 5.

This result is in accordance with previous reports accounting for blueshift suppression in similar oxygen-free

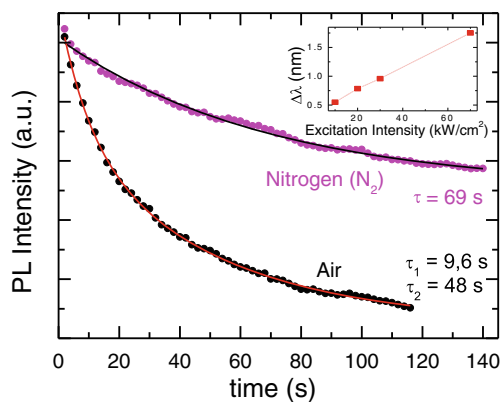


**Fig. 5** Exponential decrease of the emission intensity with excitation time, in a region of low concentration of nanocrystals deposited on  $\text{Si}_3\text{N}_4$ , in air and in a dry nitrogen atmosphere. Excitation power is  $30 \text{ kW/cm}^2$  for both measurements. Inset: Blueshift is suppressed at the center region of the nanocrystal dried drop under a dry nitrogen atmosphere, since there is no oxygen at the center of the drop for the photo-oxidation to occur

environments [44]. It is also interesting to note in Fig. 5 that to obtain a good fit to the photoluminescence decrease with the sample in air it is necessary to assume a biexponential decay. This indicates that there are two mechanisms responsible for the decay. We attribute the fast decay process to the core photo-oxidation and the slower mechanism to other processes, such as the laser induced agglomeration of nanoparticles and thermal effects. In a dry  $N_2$  atmosphere the fast decay process is suppressed and a good fit is obtained with a single exponential.

## Conclusion

We have presented data showing that photoluminescence spectra of the same set of CdTe/CdS nanocrystals may undergo either a blueshift or a redshift, depending on the power of the excitation laser. A transition between these two regimes was observed when the samples were drop cast to a silicon nitride substrate and the experiments were run at room temperature. At low-power excitation such nanoparticles are subjected to a wavelength blueshift of their emission spectrum. A redshift regime is observed for high-power excitation (intensities typically greater than  $30 \text{ kW/cm}^2$ ). Experiments performed on a dry  $N_2$  atmosphere corroborates our hypothesis that the process responsible for the blueshift is the photo-oxidation of the CdTe core, while the redshift is related to agglomeration effects of the nanocrystals, being more pronounced at regions of higher density of nanocrystals at the rim of a dried out drop deposited on  $Si_3N_4$ . Thermal expansion of the nanocrystals, caused by temperature changes due to laser heating, also contributes to the emission wavelength redshift observed at high-powers. An exponential decrease of the emission intensity was also observed. Core photo-oxidation, besides its part in the spectral shift, is also one of the mechanisms responsible for this decay and it is completely suppressed in a dry nitrogen atmosphere. Other processes concur to the decrease of the nanocrystals emission intensity over time, such as laser induced solvent evaporation and the consequent agglomeration of nanoparticles.

All the effects reported here must be taken into account when employing these colloidal quantum dots as sources of light for experiments, for example, in Cavity Quantum Electrodynamics, since this requires their deposition on a solid surface. This is even more relevant if experiments are to be conducted at room temperature, since efficient photoluminescence at high temperatures is one advantage of such nanoparticles in comparison to more traditional semiconductor quantum dots embedded in bulk material. On the other hand, once laser induced blueshifts and redshifts have been properly characterized for a given batch of nanoparticles, one could envision using controlled exposure as means of fine-

tuning the emission wavelength to bring it into resonance with an optical cavity.

**Acknowledgments** Financial support for this work was provided by Coordenação de Aperfeiçoamento de Pessoal de Nível Superior (CAPES), Conselho Nacional de Desenvolvimento Científico e Tecnológico (CNPq), Fundação de Amparo à Ciência e Tecnologia do Estado de Minas Gerais (FAPEMIG), Fundação de Amparo à Ciência e Tecnologia do Estado de Pernambuco (FACEPE) and Instituto Nacional de Ciência e Tecnologia de Fotônica (INFo). We are grateful to Prof. Beate S. Santos and Prof. Adriana Fontes of research group in Biomedical Nanotechnology (NanoBio) at Universidade Federal de Pernambuco, Brazil, for the samples used in this work.

**Conflict of Interest** The authors declare that they have no conflict of interest.

## References

- Chan WC, Nie S (1998) Quantum dot bioconjugates for ultrasensitive nonisotopic detection. *Science* 281(5385):2016–2018
- Qualtieri A, Pisanello F, Grande M, Stomeo T, Martiradonna L, Epifani G, Fiore A, Passaseo A, De Vittorio M (2010) Emission control of colloidal nanocrystals embedded in  $Si_3N_4$  photonic crystal H1 nanocavities. *Microelectron Eng* 87(5):1435–1438
- Schreder B, Schmidt T, Ptatschek V, Winkler U, Materny A, Umbach E, Lerch M, Müller G, Kiefer W, Spanhel L (2000) CdTe/CdS clusters with “core-shell” structure in colloids and films: the path of formation and thermal breakup. *J Phys Chem B* 104(8):1677–1685
- Borchert H, Talapin DV, Gaponik N, McGinley C, Adam S, Lobo A, Möller T, Weller H (2003) Relations between the photoluminescence efficiency of CdTe nanocrystals and their surface properties revealed by synchrotron XPS. *J Phys Chem B* 107(36):9662–9668
- Peng H, Zhang L, Soeller C, Travas-Sejdic J (2007) Preparation of water-soluble CdTe/CdS core/shell quantum dots with enhanced photostability. *J Lumin* 127(2):721–726
- Zeng Q, Kong X, Sun Y, Zhang Y, Tu L, Zhao J, Zhang H (2008) Synthesis and optical properties of type II CdTe/CdS core/shell quantum dots in aqueous solution via successive ion layer adsorption and reaction. *J Phys Chem C* 112(23):8587–8593
- Yan Y, Wang L, Vaughn CB, Chen G, Van Patten PG (2011) Spectroscopic investigation of oxygen sensitivity in CdTe and CdTe/CdS nanocrystals. *J Phys Chem C* 115(50):24521–24527
- Baslak C, Kus M, Cengeloglu Y, Ersoz M (2014) A comparative study on fluorescence quenching of CdTe nanocrystals with a serial of polycyclic aromatic hydrocarbons. *J Lumin* 153:177–181
- Farkhani SM, Valizadeh A (2014) Review: three synthesis methods of CdX (X= Se, S or Te) quantum dots. *IET Nanobiotechnol* 8(2):59–76
- Zhu Y, Li Z, Chen M, Cooper HM, Lu GQM, Xu ZP (2013) One-pot preparation of highly fluorescent cadmium telluride/cadmium sulfide quantum dots under neutral-pH condition for biological applications. *J Colloid Interface Sci* 390(1):3–10
- Liu YF, Xie B, Yin ZG, Fang SM, Zhao JB (2010) Synthesis of highly stable CdTe/CdS quantum dots with biocompatibility. *Eur J Inorg Chem* 2010(10):1501–1506
- Poderys V, Matulionyte M, Selskis A, Rotomskis R (2011) Interaction of water-soluble CdTe quantum dots with bovine serum albumin. *Nanoscale Res Lett* 6(1):9–14

13. Piner RD, Zhu J, Xu F, Hong S, Mirkin CA (1999) “Dip-pen” nanolithography. *Science* 283(5402):661–663
14. Gokarna A, Lee S-K, Hwang J-S, Cho Y-H, Lim YT, Chung BH, Lee M (2008) Fabrication of CdSe/ZnS quantum-dot-conjugated protein microarrays and nanoarrays
15. Roy D, Munz M, Colombi P, Bhattacharyya S, Salvétat J-P, Cumpson P, Saboungi M-L (2007) Directly writing with nanoparticles at the nanoscale using dip-pen nanolithography. *Appl Surf Sci* 254(5):1394–1398
16. Zhang (2006) Time-dependent photoluminescence blue shift of the quantum dots in living cells: effect of oxidation by singlet oxygen. *J Am Chem Soc* 128:13369–13401
17. Liu Y-S, Sun Y, Vernier PT, Liang C-H, Chong SYC, Gundersen MA (2007) pH-sensitive photoluminescence of CdSe/ZnSe/ZnS quantum dots in human ovarian cancer cells. *J Phys Chem C* 111(7):2872–2878
18. Saad A, Bakr M, Azzouz I, Kana MTA (2011) Effect of temperature and pumping power on the photoluminescence properties of type-II CdTe/CdSe core-shell QDs. *Appl Surf Sci* 257(20):8634–8639
19. Cui X, Guo H, Hou C, Gao F, Wei W, Peng B (2014) Enhanced near infrared luminescence efficiency of ligand-free LaF<sub>3</sub>:Nd/LaF<sub>3</sub> core/shell nanocrystals in solvent dispersion. *J Lumin* 154:155–159
20. Kurbanov S, Kang T (2015) Effect of ultraviolet-illumination and sample ambient on photoluminescence from zinc oxide nanocrystals. *J Lumin* 158:99–102
21. Deegan RD, Bakajin O, Dupont TF, Huber G, Nagel SR, Witten TA (1997) Capillary flow as the cause of ring stains from dried liquid drops. *Nature* 389(6653):827–829
22. Rabani E, Reichman DR, Geissler PL, Brus LE (2003) Drying-mediated self-assembly of nanoparticles. *Nature* 426(6964):271–274
23. Biju V, Makita Y, Sonoda A, Yokoyama H, Baba Y, Ishikawa M (2005) Temperature-sensitive photoluminescence of CdSe quantum dot clusters. *J Phys Chem B* 109(29):13899–13905
24. Korala L, Wang Z, Liu Y, Maldonado S, Brock SL (2013) Uniform thin films of CdSe and CdSe (ZnS) core (Shell) quantum dots by sol-gel assembly: enabling photoelectrochemical characterization and electronic applications. *ACS Nano* 7(2):1215–1223
25. Visoly-Fisher I, Dobson KD, Nair J, Bezalel E, Hodes G, Cahen D (2003) Factors affecting the stability of CdTe/CdS solar cells deduced from stress tests at elevated temperature. *Adv Funct Mater* 13(4):289–299
26. Santos (2008) Semiconductor quantum dots for biological applications. *Handbook of Self Assembled Semiconductor Nanostructures Novel Devices in Photonics and Electronic*. Elsevier
27. Andrade CG, Cabral Filho PE, Tenório DP, Santos BS, Beltrão EI, Fontes A, Carvalho LB Jr (2013) Evaluation of glycophenotype in breast cancer by quantum dot-lectin histochemistry. *Int J Nanomedicine* 8:4623
28. Ying E, Li D, Guo S, Dong S, Wang J (2008) Synthesis and bio-imaging application of highly luminescent mercaptosuccinic acid-coated CdTe nanocrystals. *PLoS One* 3(5):e2222
29. Santos B, Farias P, Menezes F, Brasil A, Fontes A, Romão L, Amaral J, Moura-Neto V, Tenorio D, Cesar C (2008) New highly fluorescent biolabels based on II–VI semiconductor hybrid organic–inorganic nanostructures for bioimaging. *Appl Surf Sci* 255(3):790–792
30. Poirier D, Weaver J (1993) CdS by XPS. *Surf Sci Spectra* 2(3):249–255
31. Lee H, Issam A, Belmahi M, Assouar M, Rinnert H, Alnot M (2009) Synthesis and characterizations of bare CdS nanocrystals using chemical precipitation method for photoluminescence application. *J Nanomaterials* 2009:41
32. Nanda J, Kuruvilla BA, Sarma D (1999) Photoelectron spectroscopic study of CdS nanocrystallites. *Phys Rev B* 59(11):7473
33. Dai M-Q, Zheng W, Huang Z, Yung L-YL (2012) Aqueous phase synthesis of widely tunable photoluminescence emission CdTe/CdS core/shell quantum dots under a totally ambient atmosphere. *J Mater Chem* 22(32):16336–16345
34. Dagtepe P, Chikan V, Jasinski J, Leppert VJ (2007) Quantized growth of CdTe quantum dots; observation of magic-sized CdTe quantum dots. *J Phys Chem C* 111(41):14977–14983
35. Yu WW, Qu L, Guo W, Peng X (2003) Experimental determination of the extinction coefficient of CdTe, CdSe, and CdS nanocrystals. *Chem Mater* 15(14):2854–2860
36. Kraus RM, Lagoudakis PG, Müller J, Rogach AL, Lupton JM, Feldmann J, Talapin DV, Weller H (2005) Interplay between Auger and ionization processes in nanocrystal quantum dots. *J Phys Chem B* 109(39):18214–18217
37. Emin S, Loukanov A, Wakasa M, Nakabayashi S, Kaneko Y (2010) Photostability of water-dispersible CdTe quantum dots: capping ligands and oxygen. *Chem Lett* 39(6):654–656
38. Ma J, Chen J-Y, Guo J, Wang C, Yang W, Xu L, Wang P (2006) Photostability of thiol-capped CdTe quantum dots in living cells: the effect of photo-oxidation. *Nanotechnology* 17(9):2083
39. Yan Y, Chen G, Van Patten PG (2011) Ultrafast exciton dynamics in CdTe nanocrystals and core/shell CdTe/CdS nanocrystals. *J Phys Chem C* 115(46):22717–22728
40. Kim (2003) Contribution of the Loss of Nanocrystal Ligands to Interdot Coupling in Films of Small CdSe/1-Thioglycerol Nanocrystals. *J Phys Chem B* 107:6318–6323
41. Fonthal G, Tirado-Mejia L, Marin-Hurtado J, Ariza-Calderon H, Mendoza-Alvarez J (2000) Temperature dependence of the band gap energy of crystalline CdTe. *J Phys Chem Solid* 61(4):579–583
42. Allahverdi Ç, Yükselici M (2008) Temperature dependence of absorption band edge of CdTe nanocrystals in glass. *New J Phys* 10(10):103029
43. Boev V, Filonovich S, Vasilevskiy M, Silva C, Gomes M, Talapin D, Rogach A (2003) Dipole–dipole interaction effect on the optical response of quantum dot ensembles. *Phys B Condens Matter* 338(1):347–352
44. van Sark WG, Frederix PL, Van den Heuvel DJ, Gerritsen HC, Bol AA, van Lingen JN, de Mello DC, Meijerink A (2001) Photooxidation and photobleaching of single CdSe/ZnS quantum dots probed by room-temperature time-resolved spectroscopy. *J Phys Chem B* 105(35):8281–8284